Autonomic Healing of Carbon Fiber/Epoxy Interfaces

Amanda R. Jones,[†] Alicia Cintora,[‡] Scott R. White,[§,⊥] and Nancy R. Sottos*,[‡,⊥]

[†]Department of Mechanical Science and Engineering, [‡]Department of Material Science and Engineering, [§]Department of Aerospace Engineering, and [⊥]Beckman Institute of Science and Technology, University of Illinois at Urbana—Champaign

ABSTRACT: A maximum of 91% recovery of interfacial shear strength (IFSS) is achieved for carbon fiber/epoxy interfaces functionalized with capsules containing reactive epoxy resin and ethyl phenyl acetate (EPA). We find a binder is necessary to improve the retention of capsules on the carbon fiber surface. Two different methods for applying the binder to the carbon fiber surface are investigated. Healing efficiency is assessed by recovery of IFSS of a single functionalized fiber embedded in a microdroplet of epoxy. Debonding of the fiber/matrix interface ruptures the capsules, releasing resin and EPA solvent into the crack plane. The solvent swells the matrix, initiating transport of residual amine functionality from the matrix for further curing with the epoxy resin delivered to the crack plane. The two binder protocols produce comparable results, both yielding higher recovery of IFSS than samples prepared without a binder.
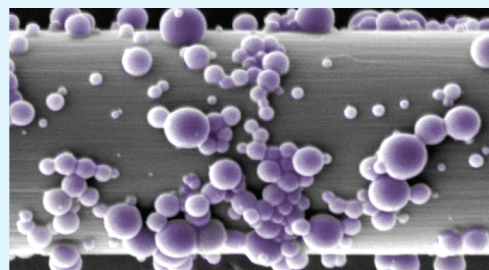
KEYWORDS: self-healing, polymer matrix composite (PMC), fiber/matrix bond, capsule

1. INTRODUCTION

The heterogeneous microstructure of fiber-reinforced composites leads to complex damage modes that are difficult to detect and costly to repair. Although there has been remarkable progress in self-healing polymers over the past decade, the ability to repair damage in fiber-reinforced composites continues to present significant technical challenges. Self-healing in fiber-reinforced composites has stringent requirements that include seamless integration with the fiber architecture, survival of the manufacturing process, and retention of original mechanical properties.

Three different healing approaches have emerged for fiber-reinforced composites: (1) capsule-based delivery of healing agents, (2) microvascular-based delivery of healing agents, and (3) thermally induced intrinsic healing. Each approach differs by the mechanism used to sequester the healing functionality until triggered by damage.[1] Capsule-based self-healing relies on damage triggered release of healing agents stored within a polymeric shell wall and has been successfully applied to bulk polymers,[2−19] polymer coatings,[20−22] fiber-reinforced polymeric composites,[5−27] and cementitious materials.[28] After release, the local healing agent is depleted, leading to only a singular, local healing event.

In vascular self-healing materials, healing agents are delivered to a damage site by a network of capillaries or hollow channels, which may be interconnected one-dimensionally (1D), two-dimensionally (2D), or three-dimensionally (3D).[29−39] The ability to circulate and replenish healing agents enables multiple healing cycles of relatively large damage volumes.

Intrinsic self-healing materials do not have a sequestered healing agent, but possess a latent self-healing functionality that is activated by damage or by an external stimulus. Bergman and Wudl[40] have reviewed both covalent and noncovalent-based intrinsic healing in polymers. One of the most studied examples of an intrinsic colvent-bond healing scheme relies on thermoreversible Diels—Alder reactions.[41−45] Intrinsic healing in supramolecular polymers depends on noncovalent interactions such as hydrogen bonding, metal—ligand bonds, and ionomeric bonding.[46−51] The bonding is reversible and these materials are capable of multiple healing cycles, but often require additional energy such as heat, pressure, or light.

In this work, a capsule-based approach is selected for autonomous recovery of interfacial shear strength (IFSS). Coalescence of interfacial damage can lead to macroscopic cracking and ultimately failure of the composite.[25] Numerous variables effect the fiber/matrix interface, including fiber and matrix mechanical properties, fiber surface treatment or sizing, surface roughness of the fiber, and cure of the epoxy matrix.[52] Fiber/matrix debonding prevents efficient load transfer between the fiber reinforcement and the polymer matrix, leading to a loss in stiffness and strength.[23] Self-healing of the fiber/matrix interfacial bond has the potential to halt or slow large-scale damage from developing. The small damage volume associated with interfacial debonding allows for the use of submicrometer capsules, which can be incorporated into the matrix interstitial regions, maintaining a relatively high fiber volume fraction in the composite.[13]

Several interfacial healing schemes have been reported in the literature. Peterson et al.[41] developed a successful remendable approach to heal interfacial damage. Maliemide-functionalized single glass fibers in a furan-functionalized epoxy were able to

recover an average of 41% after heat treatment, defined as the ratio of healed peak load minus the frictional forces divided by the virgin peak load minus the frictional forces. Sanada et al.[4] surrounded a single glass fiber with 200 μm diameter dicyclopentadiene (DCPD) filled capsules and solid particles of first-generation Grubbs' catalyst. Minimal recovery of IFSS (ca. 10%) was achieved for high loadings of capsules (ca. 40 wt %). Blaiszik et al.[23] obtained significantly higher healing efficiencies (ca. 44%) by reducing the size of the microcapsules by an order of magnitude (ca. 1.5 μm)[13] and functionalizing both catalyst and microcapsules directly on the surface of a glass fiber. Here, healing efficiency was defined as the ratio of healed peak load to virgin peak load, which was also adopted in this work. Using an encapsulated resin-solvent healing chemistry functionalized on glass fibers, Jones et al.[24] achieved full recovery of IFSS (100% healing efficiency) and demonstrated healing with capsules as small as 600 nm in diameter.

Here, we apply the encapsulated resin-solvent healing chemistry[24] for autonomous repair of the interface between a carbon fiber and an epoxy matrix. Self-healing of the carbon fiber/epoxy interface is challenging because of the size scale of carbon fibers (ca. 5 μm in diameter) and the electrokinetic potential of carbon fibers in comparison to glass fibers. Sized glass fibers possess a positive zeta potential, whereas the electrical charge of sized carbon fibers is neutral or negative.[53] Although capsules have a high affinity for the glass fiber surface,[24] an additional binder is necessary to stabilize capsules at the carbon fiber/matrix interface.

Techniques for measuring interfacial bond strength include fiber pull-out,[54−56] fiber push-out,[57−61] and fiber fragmentation.[62−66] For evaluation of healing, we adopt a single fiber pull-out protocol using the microbond specimen geometry first developed by Miller et al.[67] to obtain virgin IFSS and subsequent recovery. In this technique, a single carbon fiber is embedded in a microdroplet of resin as shown in Figure 1.
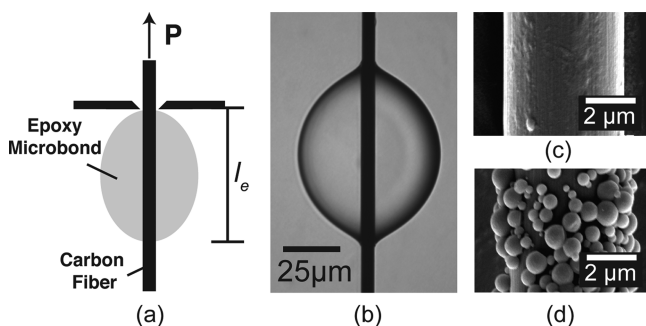

Figure 1. Single fiber microbond specimens. (a) Schematic of a microbond test configuration and (b) optical micrograph of a carbon fiber/epoxy microbond. (c) Scanning electron microscopy (SEM) of a plain carbon fiber surface used in a control specimen, and (d) SEM of a carbon fiber for a self-healing specimen.

The IFSS is obtained by constraining the microdroplet and pulling the fiber in tension until complete interfacial debonding is achieved. Microbond specimens are then retested to evaluate healing performance. Self-healing functionality is added to the specimens by functionalizing carbon fibers with both a binder and submicrometer capsules. We examine two different binder techniques and the effect of capsule concentration on recovery of IFSS.

2. MATERIALS AND METHODS

2.1. Encapsulation of Healing Agents. Capsules containing a resin-solvent solution were prepared by in situ polymerization of urea-formaldehyde (UF) as described in prior work.[24] The core solution contained a mixture of 2.5 wt % hexadecane, an ultrahydrophobe, and a 30:70 ratio by weight of EPON 862 (diglycidyl ether of bisphenol-F):ethyl phenyl acetate (EPA). This core solution was slowly added to a 30 mL aqueous solution of approximately 1.25 wt % ethylene maleic anhydride copolymer (ZeMac 400 EMA, Vertellus), 0.45 g of urea, 0.1 g of ammonium chloride, and 0.045 g of resorcinol under mechanical agitation at 800 rpm. The mixture was allowed to equilibrate for 10 min before sonication. A 3.2 mm tapered tip of a 750 W Ultrasonic Homogenizer (Cole-Parmer) was used at 40% intensity with a 0.2 s pulsing parameter for 1 min. Formalin (1.2 g) was then added to the encapsulation and the temperature of the control bath was increased to 55 °C at 1 °C/min and held for 4 h. Capsules were centrifuged to remove excess surfactant and used in an aqueous solution to size carbon fibers. EPON 862 was purchased from Miller-Stephenson. EPA, urea, ammonium chloride, and resorcinol were purchased from Sigma Aldrich.

2.2. Fiber Functionalization. Carbon fibers with a proprietary epoxy-compatible sizing were obtained from Hexcel (IM7-G). Single carbon fibers were isolated from a fiber tow and the fiber surface was decorated with capsules using a dip coat technique. In contrast to glass fibers,[23,24] a binder was required to keep capsules at the carbon fiber/epoxy interface and to achieve repeatable healing performance. Two different methods, summarized in Figure 2, were developed to apply
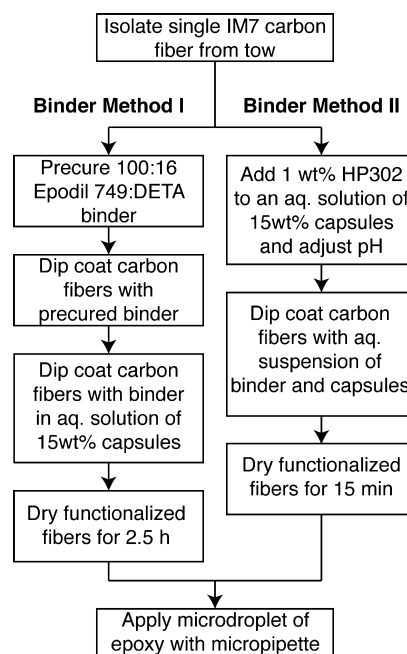

Figure 2. Methods for applying binder and capsules to the carbon fiber surface.

the binder to the carbon fiber surface. In the first method, binder method I, a stoichiometric mixture of Epodil 749 (Momentive), an epoxy diluent, and diethyltriamine (DETA, Sigma Aldrich) was prepared. The binder was allowed to precure before single carbon fibers were dipped in the mixture. Coated single carbon fibers were then immediately dipped into an aqueous suspension of capsules at a known concentration (varied from 5 to 15 wt %).

In binder method II, an aqueous suspension of phenoxy (HP302, Michelman, Inc.) was combined with an aqueous capsule solution of known concentration. The binder concentration was varied from 1 to 4 wt % of the capsule solution, with 1 wt % yielding the most consistent coverage. The wt % total solids was varied from 5 to 25 wt % with 15 wt % yielding the highest coverages while minimizing

agglomerations of capsules. The pH of the solution was critical for consistent, even coverage and was adjusted to 3.6 using solutions of HCl and NaOH.

For both methods, the capsule coverage, ξ, is defined as the surface area of capsules on the surface of the fiber divided by the surface area of the fiber, or

$$\xi \approx \frac{N\pi r_{cap}^2}{\pi d l_e} \qquad (1)$$

where N is the number of capsules present on the surface of the fiber, r_{cap} is the radius of the capsule, d is the diameter of the fiber, and l_e is the embedded length of the fiber in the microbond specimen.[24] Capsule coverage, ξ, is measured by image analysis of SEM micrographs.

2.3. Microbond Specimen Preparation. Microbond specimens consisted of a single carbon fiber embedded in an epoxy droplet as shown in Figure 1. For binder method I, capsule-functionalized fibers were allowed to dry for 2.5 h before application of the epoxy microbond to keep the degree of cure of the binder consistent. For binder method II, only 15 min was required to remove excess water because functionalization was not dependent on a precure time. Three types of control specimens were prepared in a similar fashion. The first control (C0) consisted of an as-received carbon fiber (no binder, no capsules) embedded in an epoxy droplet. For the other two controls (CI and CII), carbon fibers were prepared with binder alone but no capsules.

A micropipette was used to apply a bead of epoxy (80−130 μm in length) to either as-received or capsule-functionalized fibers. EPON 828 (diglycidyl ether of bisphenol A) resin and DETA (diethylenetriamine), an aerospace grade epoxy with high bond strength, was mixed at 12 pph DETA to EPON 828, degassed and allowed to react at room temperature for 1 h before being applied to the fibers. The specimens were cured at room temperature for 24 h and then at 35 °C for 24 h. This cure cycle resulted in a slightly undercured (ca. 80%) matrix with residual functionality.

2.4. Microbond Test Method. After curing, the embedded fiber length (l_e) of each specimen was measured optically (Figure 1). The samples were tested with a custom-built load frame as described by Jones et al.[24] and imaged simultaneously through a zoom lens (Navitar) to observe interfacial debonding. Samples were loaded in displacement control using a linear actuator (Physik Instrumente) translating at a rate of 0.5 μm/s and controlled through LabView (National Instruments, v10.0). Force was measured with a 150 g load cell (Honeywell Sensotec). Samples were tested to the maximum force (P_{max}) needed to cause full interfacial debond. After debond, the force dropped quickly and then slowly increased to a frictional plateau value ($P_{friction}$). The sample was then removed from the load frame, allowed to heal for 24 h at room temperature, and then retested following the same protocol.

The IFSS (τ) was calculated from the peak applied force (P_{max}), the fiber diameter (d), and the embedded length (l_e),

$$\tau = \frac{P_{max}}{\pi d l_e} \qquad (2)$$

The healing efficiency (η) was defined as the ratio of the recovered interfacial shear strength to the original value

$$\eta = \frac{\tau_{healed}}{\tau_{virgin}} = \frac{P_{max,healed}}{P_{max,virgin}} \qquad (3)$$

3. RESULTS AND DISCUSSION

3.1. Capsule Coverage. The capsule coverage, ξ, for binder method I, is shown in Figure 3 as a function of the binder precure time for a capsule concentration of 15 wt % in deionized water. The degree of cure of the binder before submerging in the aqueous capsule suspension was critical to achieve consistent coverage. Immediately after mixing the
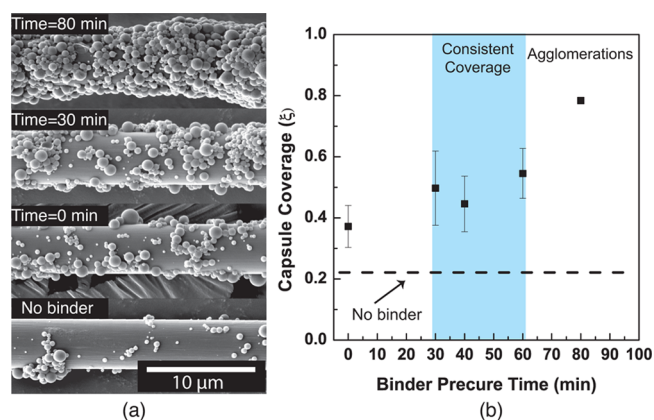

Figure 3. Capsule coverage for binder method I. (a) SEM images of carbon fibers prepared with binder method I for different binder precure time. (b) Capsule coverage, ξ, as a function of increasing binder cure time. The dashed line indicates the lower coverage resulting from carbon fibers functionalized without a binder.

amine and diluent of the binder material together (time, $t = 0$), the coverage was low but still higher than the case where no binder was used (dashed line). After 30 min of precure time the coverage increased slightly and stabilized for the next 30 min ($t = 60$ min precure time). At a binder precure time of 80 min, large agglomerations of capsules began to form and coat the single fiber. The amount of coverage varied with capsule concentration and ambient curing conditions, but the overall trend remained the same. Capsule coverage was quantified for each batch of samples.

Because of the inherent variation in binder method I and issues with cross-contamination in the second dip bath, a second binder protocol was explored. For binder method II, an aqueous suspension of binder (HP302) was combined with capsules to produce a single step water-based self-healing sizing. For this method, capsule coverage was strongly dependent on pH of the solution (Figure 4). At low pH (ca. 3.3), capsule coverage along the fiber surface was not uniform with either agglomerations of capsules or no coverage at all. As the pH increased, the capsule coverage became more consistent until higher pH values (ca. 3.9). For the pH of 3.9, the capsule coverage was negligible. The pH of the capsule solution
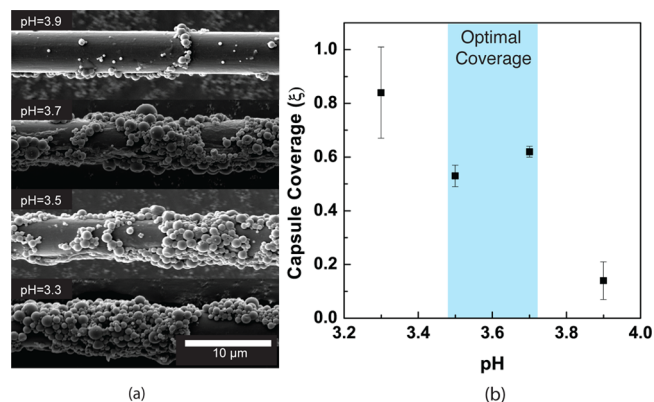

Figure 4. Capsule coverage for binder method II. (a) SEM micrographs of carbon fibers prepared with binder method II for different solution pH. (b) Capsule coverage for increasing pH of the sizing solution.

controlled the charge on the capsule surface, which affected the affinity of the capsules to the fiber surface.

3.2. Recovery of IFSS. Self-healing of the fiber/matrix interfacial bond was assessed by testing of microbond specimens. A summary of sample designations, healing performance, and IFSS values is provided in Table 1. Three

Table 1. Interfacial Strengths and Healing Efficiencies for Different Specimen Types

sample type	virgin IFSS (MPa)	healing efficiency, η	capsule coverage, ξ	no. of samples, n
C0: as received carbon fiber	44.0 ± 6.6	0.21 ± 0.05		19
CI: binder 1 only	48.7 ± 8.1	0.17 ± 0.04		11
CII: binder 2 only	47.9 ± 5.7	0.32 ± 0.08		7
SH: no binder	35.2 ± 5.2	0.25 ± 0.05	0.22	22
SHI: binder method I	41.6 ± 2.8	0.37 ± 0.02	0.34	8
	32.3 ± 2.5	0.48 ± 0.05	0.56	18
	25.7 ± 1.9	0.57 ± 0.05	0.63	21
SHII: binder method II	26.9 ± 5.4	0.83 ± 0.17	0.61	8
SH-glass[a]	32 ± 3.0	0.34 ± 0.05	0.4	12
	27 ± 3.1	0.50 ± 0.05	0.5	10
	23 ± 1.3	0.60 ± 0.08	0.7	11

[a]Results from Jones et al.[24] with the same capsule size and core content are shown in comparison to current work. The difference in IFSS is due to superior bonding between the carbon fibers and epoxy microdroplet when compared to glass fibers.

different controls were tested to evaluate first the baseline bond strength of a carbon fiber embedded in epoxy (C0), as well as the effect of each of the binders alone on the IFSS (CI and CII). Self-healing specimens were prepared without any binder (SH), with binder method I at multiple coverages (SHI) and with Binder Method II at a capsule coverage of ξ = 0.6 (SHII). Results from Jones et al.,[24] for glass fibers functionalized with similar capsules, but no binder, and embedded in the same epoxy droplet are included for comparison.

A representative load−displacement curve is shown in Figure 5a for a self-healing specimen (binder method I) with a high capsule coverage (ca. ξ = 0.6). The sample was loaded to 50 mN (P_{max}), at which point full interfacial debonding occurred.

The load then dropped and quickly reached a frictional plateau of 15 mN ($P_{friction}$). Ruptured capsules released the resin-solvent healing agent into the crack plane. The solvent swelled the matrix, pulling residual functionality to the crack plane that reacted with the coencapsulated resin, and formed a healed film. After 24 h, the sample was retested and ca. 75% recovery of IFSS was achieved for select samples. Since the amount of solvent released is small, we believe the swelling is highly localized and with time the solvent evaporates leaving little residual effect on the matrix properties. Both Caruso[12] and Jones[24] achieved full recovery of mechanical properties suggesting no degradation of the matrix material from the solvent.

Control specimens (C0), consisting of an as-received carbon fiber embedded in the same epoxy matrix, only recovered the frictional force (η = 0.21) 24 h after initial testing (Figure 5b). As summarized in Table 1, control specimens, CI and CII, with binder but no capsules also only recovered the frictional force. In both cases though, the addition of the binder improved the interface strength. In prior work with glass fibers, two additional controls were explored: microencapsulated DCPD monomer and pure EPA. Although DCPD monomer is not a solvent, it has potential to swell the epoxy similar to EPA, but without catalyst, has no healing ability. Blaiszik et al.[23] reports that healing efficiency of specimens prepared with DCPD capsule functionalized fibers is within experimental error of specimens prepared with plain as-received glass fibers (no healing effect). Jones et al.[24] shows that healing efficiency for specimens prepared with EPA alone is well above (η = 0.72) the frictional recovery of plain glass fibers (η = 0.24).

3.3. Effect of Capsule Coverage. Three different capsule coverages were investigated (ξ = 0.34, 0.56, 0.63) for binder method I. The effect of capsule coverage on healing efficiency is summarized in Figure 6 and compared to previous results for similar glass fiber specimens.[24] Capsule coverage was quantified prior to application of the epoxy microdroplet and healing performance was used to evaluate the ability of the binder to effectively adhere capsules to the interface. Higher capsule coverages result in more healing agent delivered to the crack plane and higher healing efficiencies. The healing performance of binder method I is remarkably similar to the results for glass fiber specimens prepared with submicrometer (ca. 0.6 μm in diameter) capsules, suggesting that the healing chemistry is
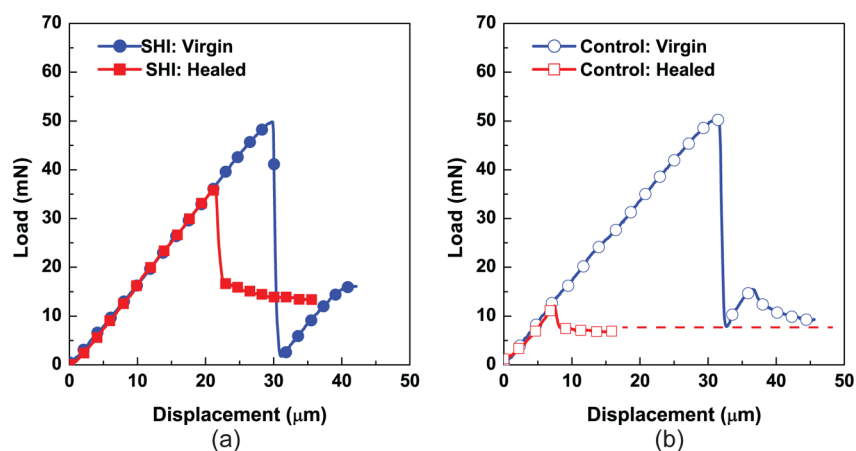

Figure 5. Representative load−displacement curves for microbond testing of (a) self-healing (SHI) specimens prepared with binder method I demonstrating η = 75% recovery of IFSS and (b) a control specimen consisting of a plain carbon fiber (C0) embedded in epoxy, which only recovers frictional force.
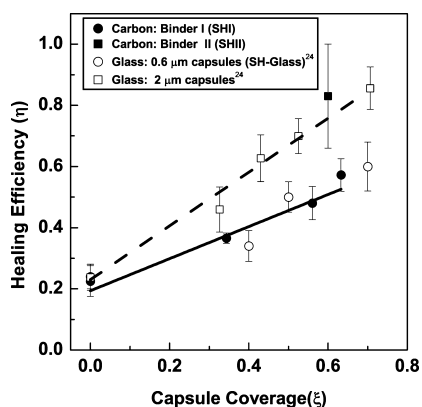
Figure 6. Healing efficiency as a function of capsule coverage for carbon fiber specimens prepared with binder method I, binder method II, and results for glass fiber microbond specimens from Jones et al.[24] Error bars are 95% confidence interval.

effective for multiple fiber/epoxy systems. Binder method II produced even higher healing performance when compared to binder method I and glass fiber specimens prepared with similar microcapsules (0.6 μm in diameter). We hypothesize the improvement in healing efficiency from binder method I to binder method II is likely related to high capsule coverage that remains at the interface after application of the microdroplet of epoxy. For comparison, glass fiber microbond specimens prepared with larger microcapsules (ca. 2 μm in diameter) are also included and represent the highest interfacial healing performance obtained with this chemistry.[24]

The effect of capsule coverage on virgin IFSS is also reported in Table 1. At low concentrations ($\xi = 0.34$), the addition of capsules minimally affected the virgin IFSS. The average IFSS was below the virgin IFSS of an as-received carbon fiber/epoxy microbond (C0), but within the experimental error of this control specimen. This result differs from our previous work with glass fiber/epoxy microbonds where a low capsule coverage led to a modest increase in virgin IFSS.[24] Further increases in capsule coverage ($\xi = 0.56$) caused a reduction in IFSS due to less available surface area for the matrix to bond to the fiber. At the highest capsule coverage ($\xi = 0.63$), there was a more significant loss of IFSS, but healing performance was maximized. This trade off between high healing performance and high virgin IFSS was observed for both carbon and glass fiber/epoxy microbonds. Virgin IFSS of self-healing carbon fiber/epoxy microbonds will likely be improved with a different binder or a more uniform method of applying the capsules to the fiber surface.

3.4. Effect of Binder Method. Healing performance for the different binder methods is compared in Figure 7. Carbon fiber/epoxy microbond specimens prepared without a binder had significantly lower capsule coverage, and therefore had reduced healing performance. The addition of the binder increased the capsule coverage and also aided in keeping capsules adhered to the fiber during microbond application. Maximum healing performance increased to 57%, for binder method I, whereas for binder method II, the average healing efficiency further increased to ca. 80%. We hypothesize this is due to the lack of cross contamination between the two dip baths used in binder method I, which impeded the consistency of coverage. We anticipate further increases in healing efficiency may result from adjusting the ratio of solvent to resin
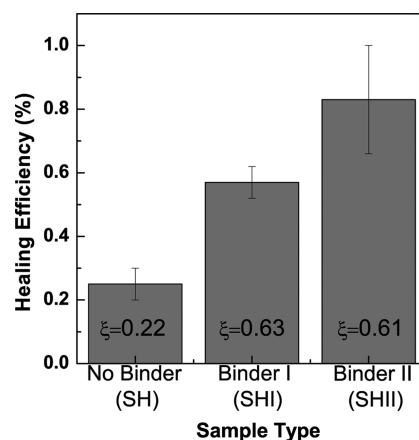

Figure 7. Comparison of binder method I (SHI) and binder method II (SHII) at the same capsule coverage ($\xi \approx 0.6$) and samples prepared without binder (SH, $\xi = 0.22$). The capsule coverage for samples prepared without binder is significantly lower than for samples prepared with a binder technique, which leads to a reduced healing performance for samples without binder. Error bars are 95% confidence interval.

encapsulated and improving the consistency of capsule coverage.

4. CONCLUSIONS

Autonomous repair of a high-performance carbon fiber/epoxy interface was achieved with a maximum of 91% recovery. Healing efficiencies increased with higher capsule coverage, but the virgin IFSS decreased due to reduced surface area for bonding. The application of binder was critical for stabilizing capsules at the interface. Healing results using binder method I and carbon fibers with an commercial epoxy-based sizing (IM7-G) were very similar to the healing performance of a glass fiber with an aminopropylsilane (APS)-based sizing suggesting that the resin-solvent healing chemistry can be applied over a wide range of fiber/matrix interfaces. Healing performance was maximized with binder method II due to the high coverage of capsules that remains on the fiber interface during specimen manufacture. Future work will be aimed at optimization of the coating methods for compatibility with composite prepregging techniques.

■ AUTHOR INFORMATION

Corresponding Author
*E-mail: n-sottos@illinois.edu.

Notes
The authors declare no competing financial interest.

■ ACKNOWLEDGMENTS

■ REFERENCES

(1) Blaiszik, B.; Kramer, S.; Olugebefola, S.; Moore, J.; Sottos, N.; White, S. Self-healing Polymers and Composites. *Annu. Rev. Mater. Res.* **2010**, *40*, 179–211.

(2) White, S. R.; Sottos, N. R.; Geubelle, P. H.; Moore, J. S.; Kessler, M. R.; Sriram, S. R.; Brown, E. N.; Viswanathan, S. Autonomic Healing of Polymer Composites. *Nature* **2001**, *409*, 794−797.

(3) Brown, E.; White, S.; Sottos, N. Retardation and Repair of Fatigue Cracks in a Microcapsule Toughened Epoxy Composite-Part II: In Situ Self-healing. *Compos. Sci. Technol.* **2005**, *65*, 2474−2480.

(4) Sanada, K.; Yasuda, I.; Shindo, Y. Transverse Tensile Strength of Unidirectional Fibre-reinforced Polymers and Self-healing of Interfacial Debonding. *Plast., Rubber Compos.* **2006**, *35*, 67−72.

(5) Blaiszik, B.; Caruso, M.; McIlroy, D.; Moore, J.; White, S.; Sottos, N. Microcapsules Filled with Reactive Solutions for Self-healing Materials. *Polymer* **2009**, *50*, 990−997.

(6) Xiao, D. S.; Yuan, Y. C.; Rong, M. Z.; Zhang, M. Q. Self-healing Epoxy Based on Cationic Chain Polymerization. *Polymer* **2009**, *50*, 2967−2975.

(7) Keller, M. W.; White, S. R.; Sottos, N. R. A Self-healing Poly (Dimethyl Siloxane) Elastomer. *Adv. Funct. Mater.* **2007**, *17*, 2399−2404.

(8) Yuan, Y. C.; Rong, M. Z.; Zhang, M. Q.; Chen, J.; Yang, G. C.; Li, X. M. Self-healing Polymeric Materials Using Epoxy/Mercaptan as the Healant. *Macromolecules* **2008**, *41*, 5197−5202.

(9) Jin, H.; Mangun, C. L.; Stradley, D. S.; Moore, J. S.; Sottos, N. R.; White, S. R. Self-healing Thermoset Using Encapsulated Epoxy-Amine Healing Chemistry. *Polymer* **2012**, *53*, 581−587.

(10) Jin, H.; Mangun, C. L.; Griffin, A. S.; Moore, J. S.; Sottos, N. R.; White, S. R. Thermally Stable Autonomic Healing in Epoxy Using a Dual-Microcapsule System. *Adv. Mater.* **2013**, *26*, 1−6.

(11) Yin, T.; Zhou, L.; Rong, M. Z.; Zhang, M. Q. Self-healing Woven Glass Fabric/Epoxy Composites with the Healant Consisting of Micro-Encapsulated Epoxy and Latent Curing Agent. *Smart Mater. Struct.* **2008**, *17*, 015019.

(12) Caruso, M. M.; Blaiszik, B. J.; White, S. R.; Sottos, N. R.; Moore, J. S. Full Recovery of Fracture Toughness Using a Nontoxic Solvent-Based Self-healing System. *Adv. Funct. Mater.* **2008**, *18*, 1898−1904.

(13) Blaiszik, B.; Sottos, N.; White, S. Nanocapsules for Self-healing Materials. *Compos. Sci. Technol.* **2008**, *68*, 978−986.

(14) Neuser, S.; Michaud, V. Fatigue Response of Solvent-Based Self-healing Smart Materials. *Exp. Mech.* **2013**, *54*, 1−12.

(15) Neuser, S.; Michaud, V.; White, S. Improving Solvent-based Self-healing Materials through Shape Memory Alloys. *Polymer* **2012**, *53*, 370−378.

(16) Cosco, S.; Ambrogi, V.; Musto, P.; Carfagna, C. Urea-Formaldehyde Microcapsules Containing an Epoxy Resin: Influence of Reaction Parameters on the Encapsulation Yield. *Macromol. Symp.* **2006**, *234*, 184−192.

(17) Mookhoek, S. D.; Blaiszik, B. J.; Fischer, H. R.; Sottos, N. R.; White, S. R.; Van Der Zwaag, S. Peripherally Decorated Binary Microcapsules containing Two Liquids. *J. Mater. Chem.* **2008**, *18*, 5390−5394.

(18) Gragert, M.; Schunack, M.; Binder, W. H. Azide/Alkyne-″Click″-Reactions of Encapsulated Reagents: Toward Self-healing Materials. *Macromol. Rapid Commun.* **2011**, *32*, 419−25.

(19) Pastine, S. J.; Okawa, D.; Zettl, A.; Fréchet, J. M. J. Chemicals On Demand with Phototriggerable Microcapsules. *J. Am. Chem. Soc.* **2009**, *131*, 13586−13587.

(20) Suryanarayana, C.; Rao, K. C.; Kumar, D. Preparation and Characterization of Microcapsules containing Linseed Oil and its Use in Self-healing Coatings. *Prog. Org. Coat.* **2008**, *63*, 72−78.

(21) Cho, S. H.; White, S. R.; Braun, P. V. Self-healing Polymer Coatings. *Adv. Mater.* **2009**, *21*, 645−649.

(22) Samadzadeh, M.; Boura, S. H.; Peikari, M.; Kasiriha, S.; Ashrafi, A. A Review on Self-healing Coatings based on Micro/Nanocapsules. *Prog. Org. Coat.* **2010**, *68*, 159−164.

(23) Blaiszik, B. J.; Baginska, M.; White, S. R.; Sottos, N. R. Autonomic Recovery of Fiber/ Matrix Interfacial Bond Strength in a Model Composite. *Adv. Funct. Mater.* **2010**, *20*, 3547−3554.

(24) Jones, A.; Blaiszik, B.; White, S.; Sottos, N. Full Recovery of Fiber/Matrix Interfacial Bond Strength Using a Microencapsulated Solvent-based Healing System. *Compos. Sci. Technol.* **2013**, *79*, 1−7.

(25) Kessler, M.; Sottos, N.; White, S. Self-healing Structural Composite Materials. *Composites, Part A* **2003**, *34*, 743−753.

(26) Moll, J. L.; Jin, H.; Mangun, C. L.; White, S. R.; Sottos, N. R. Self-sealing of Mechanical Damage in a Fully Cured Structural Composite. *Compos. Sci. Technol.* **2013**, *79*, 15−20.

(27) Patel, A. J.; Sottos, N. R.; Wetzel, E. D.; White, S. R. Autonomic Healing of Low-Velocity Impact Damage in Fiber-Reinforced Composites. *Composites, Part A* **2010**, *41*, 360−368.

(28) Van Tittelboom, K.; De Belie, N. Self-healing in Cementitious Materials-A Review. *Materials* **2013**, *6*, 2182−2217.

(29) Pang, J.; Bond, I. 'Bleeding Composites'−Damage Detection and Self-Repair using a Biomimetic Approach. *Composites, Part A* **2005**, *36*, 183−188.

(30) Trask, R.; Williams, G.; Bond, I. Bioinspired Self-healing of Advanced Composite Structures Using Hollow Glass Fibres. *J. R. Soc., Interface* **2007**, *4*, 363−371.

(31) Williams, G.; Trask, R.; Bond, I. A Self-healing Carbon Fibre Reinforced Polymer for Aerospace Applications. *Composites, Part A* **2007**, *38*, 1525−1532.

(32) Williams, H.; Trask, R.; Bond, I. Self-healing Sandwich Panels: Restoration of Compressive Strength after Impact. *Compos. Sci. Technol.* **2008**, *68*, 3171−3177.

(33) Toohey, K. S.; Sottos, N. R.; Lewis, J. A.; Moore, J. S.; White, S. R. Self-healing Materials with Microvascular Networks. *Nat. Mater.* **2007**, *6*, 581−585.

(34) Hansen, C. J.; Wu, W.; Toohey, K. S.; Sottos, N. R.; White, S. R.; Lewis, J. A. Self-healing Materials with Interpenetrating Microvascular Networks. *Adv. Mater.* **2009**, *21*, 4143−4147.

(35) Hansen, C. J.; White, S. R.; Sottos, N. R.; Lewis, J. A. Accelerated Self-healing via Ternary Interpenetrating Microvascular Networks. *Adv. Funct. Mater.* **2011**, *21*, 4320−4326.

(36) Hamilton, A. R.; Sottos, N. R.; White, S. R. Self-healing of Internal Damage in Synthetic Vascular Materials. *Adv. Mater.* **2010**, *22*, 5159−5163.

(37) Hamilton, A. R.; Sottos, N. R.; White, S. R. Pressurized Vascular Systems for Self-healing Materials. *J. R. Soc., Interface* **2011**, *9*, 1020−1028.

(38) Norris, C. J.; Meadway, G. J.; O'Sullivan, M. J.; Bond, I. P.; Trask, R. S. Self-healing Fibre Reinforced Composites via a Bioinspired Vasculature. *Adv. Funct. Mater.* **2011**, *21*, 3624−3633.

(39) Norris, C.; Bond, I.; Trask, R. Interactions between Propagating Cracks and Bioinspired Self-healing Vascules Embedded in Glass Fibre Reinforced Composites. *Compos. Sci. Technol.* **2011**, *71*, 847−853.

(40) Bergman, S. D.; Wudl, F. Mendable Polymers. *J. Mater. Chem.* **2008**, *18*, 41.

(41) Peterson, A. M.; Jensen, R. E.; Palmese, G. R. Thermoreversible and Remendable Glass-Polymer Interface for Fiber-Reinforced Composites. *Compos. Sci. Technol.* **2011**, *71*, 586−592.

(42) Peterson, A. M.; Kotthapalli, H.; Rahmathullah, M. A. M.; Palmese, G. R. Investigation of Interpenetrating Polymer Networks for Self-healing Applications. *Compos. Sci. Technol.* **2012**, *72*, 330−336.

(43) Chen, X.; Dam, M. A.; Ono, K.; Mal, A.; Shen, H.; Nutt, S. R.; Sheran, K.; Wudl, F. A Thermally Re-mendable Cross-Linked Polymeric Material. *Science (Washington, DC, U. S.)* **2002**, *295*, 1698−1702.

(44) Park, J. S.; Takahashi, K.; Guo, Z.; Wang, Y.; Bolanos, E.; Hamann-Schaffner, C.; Murphy, E.; Wudl, F.; Hahn, H. T. Towards Development of a Self-healing Composite using a Mendable Polymer and Resistive Heating. *J. Compos. Mater.* **2008**, *42*, 2869−2881.

(45) Pratama, P. A.; Peterson, A. M.; Palmese, G. R. Diffusion and Reaction Phenomena in Solution-Based Healing of Polymer Coatings Using the Diels-Alder Reaction. *Macromol. Chem. Phys.* **2012**, *213*, 173−181.

(46) Kalista, S. J.; Ward, T. C.; Oyetunji, Z. Self-healing of Poly(Ethylene-co-Methacrylic Acid) Copolymers Following Projectile Puncture. *Mech. Adv. Mater. Struct.* **2007**, *14*, 391−397.

(47) Varley, R. J.; van der Zwaag, S. Towards an Understanding of Thermally Activated Self-healing of an Ionomer System during Ballistic Penetration. *Acta Mater.* **2008**, *56*, 5737−5750.

(48) Burnworth, M.; Tang, L.; Kumpfer, J. R.; Duncan, A. J.; Beyer, F. L.; Fiore, G. L.; Rowan, S. J.; Weder, C. Optically Healable Supramolecular Polymers. *Nature* **2011**, *472*, 334−7.

(49) Cordier, P.; Tournilhac, F.; Soulie-Ziakovic, C.; Leibler, L. Self-healing and Thermoreversible Rubber from Supramolecular Assembly. *Nature* **2008**, *451*, 977−980.

(50) Corten, C. C.; Urban, M. W. Repairing Polymers Using Oscillating Magnetic Field. *Adv. Mater.* **2009**, *21*, 5011−5015.

(51) Chen, Y.; Guan, Z. Self-Assembly of Core-Shell Nanoparticles for Self-healing Materials. *Polym. Chem.* **2013**, *4*, 4885.

(52) Hughes, J. The Carbon Fibre/ Epoxy Interface−A Review. *Compos. Sci. Technol.* **1991**, *41*, 13−45.

(53) Mäder, E.; Grundke, K.; Jacobasch, H.-J.; Wachinger, G. Surface, Interphase and Composite Property Relations in Fibre-Reinforced Polymers. *Composites* **1994**, *25*, 739−744.

(54) Zhandarov, S.; Gorbatkina, Y.; Mäder, E. Adhesional Pressure as a Criterion for Interfacial Failure in Fibrous Microcomposites and its Determination Using a Microbond Test. *Compos. Sci. Technol.* **2006**, *66*, 2610−2628.

(55) Zhandarov, S.; Mäder, E. Peak Force as Function of the Embedded Length in Pull-out and Microbond Tests: Effect of Specimen Geometry. *J. Adhes. Sci. Technol.* **2005**, *19*, 817−855.

(56) Zhandarov, S.; Pisanova, E.; Schneider, K. Fiber-Stretching Test: A New Technique for Characterizing the Fiber-Matrix Interface using Direct Observation of Crack Initiation and Propagation. *J. Adhes. Sci. Technol.* **2000**, *14*, 381−398.

(57) Lin, G.; Geubelle, P.; Sottos, N. Simulation of Fiber Debonding with Friction in a Model Composite Pushout Test. *Int. J. Solids Struct.* **2001**, *38*, 8547−8562.

(58) Liang, C.; Hutchinson, J. Mechanics of the Fiber Pushout Test. *Mech. Mater.* **1993**, *14*, 207−221.

(59) Cordes, R. D.; Daniel, I. M. Determination of Interfacial Properties from Observations of Progressive Fiber Debonding and Pullout. *Compos. Eng.* **1995**, *5*, 633−648.

(60) Bechel, V. T.; Sottos, N. R. High Temperature Fiber Pushout of Pristine and Transversely Fatigued SiC/Ti-6−4. *J. Mater. Sci.* **1999**, *34*, 3471−3478.

(61) Bechel, V.; Sottos, N. Application of Debond Length Measurements to Examine the Mechanics of Fiber Pushout. *J. Mech. Phys. Solids* **1998**, *46*, 1675−1697.

(62) Yilmaz, Y. I. Analyzing Single Fiber Fragmentation Test Data by Using Stress Transfer Model. *J. Compos. Mater.* **2002**, *36*, 537−551.

(63) Gong, X. J.; Arthur, J. A.; Penn, L. S. Strain Rate Effect in the Single-Fiber-Fragmentation Test. *Polym. Compos.* **2001**, *22*, 349−360.

(64) Kim, B. W.; Nairn, J. A. Observations of Fiber Fracture and Interfacial Debonding Phenomena Using the Fragmentation Test in Single Fiber Composites. *J. Compos. Mater.* **2002**, *36*, 1825−1858.

(65) Wadsworth, N. J.; Spilling, I. Load Transfer from Broken Fibres in Composite Materials. *J. Phys. D: Appl. Phys.* **1968**, *1*, 1049−1058.

(66) Wagner, H. D.; Nairn, J. A.; Detassis, M. Toughness of Interfaces from Initial Fiber-Matrix Debonding in a Single Fiber Composite Fragmentation Test. *Appl. Compos. Mater.* **1995**, *2*, 107−117.

(67) Miller, B.; Muri, P.; Rebenfeld, L. A Microbond Method for Determination of the Shear Strength of a Fiber/ Resin Interface. *Compos. Sci. Technol.* **1987**, *28*, 17−32.